

Modelling Hydrogen Refuelling for Light-Duty Passenger Vehicles

Muhammad Atif Mahmood^{*}, Nicola Massarotti, Laura Vanoli

Department of Engineering, University of Naples "Parthenope", Naples 80143, Italy

Corresponding Author Email: muhammadatif.mahmood001@studenti.uniparthenope.it

Copyright: ©2024 The authors. This article is published by IETA and is licensed under the CC BY 4.0 license (<http://creativecommons.org/licenses/by/4.0/>).

<https://doi.org/10.18280/mmep.111005>

ABSTRACT

Received: 9 August 2024

Revised: 3 October 2024

Accepted: 10 October 2024

Available online: 31 October 2024

Keywords:

hydrogen refuelling station, refuelling performance, thermodynamic modelling, vehicle tank temperature

Due to the rising concerns over environmental issues and the pressing need to reduce carbon emissions, hydrogen (H₂) has gained significant attention as a clean, reliable and sustainable vehicle energy carrier, which is produced from renewable sources. Hydrogen Refuelling Stations (HRSs) are considered a crucial infrastructure for supporting Fuel Cell Electric Vehicles (FCEVs). Nonetheless, a significant obstacle to the commercialization of FCEVs is to store highly flammable hydrogen gas efficiently and securely. Numerous techniques for storing H₂ have been devised, however, compressed H₂ storage tanks, due to their lightweight and effectiveness, are the most used technique for storing H₂ in automobiles. In the present study, a thermodynamic model of HRS was developed to examine the effects of different refuelling parameters such as H₂ supply temperature and Average Pressure Ramp Rate (APRR) on light-duty FCEVs fueling performance, and State of Charge (SOC) for 70 MPa, 99-liter type IV H₂ cylinder. Compared to other refuelling parameters, it was observed that the hydrogen supply temperature has a significant effect on the final tank temperature and SOC. Simulation results show that an increase in H₂ supply temperature from -40°C to 20°C causes an increase of 65.2% in end gas temperature (68.9°C to 113.8°C) and 9.3% lower SOC (92.4% to 84.6%) respectively.

1. INTRODUCTION

A promising way to reduce carbon emissions in the transportation sector is to employ hydrogen (H₂) as an alternative fuel to conventional fossil fuel-based fuels (diesel and gasoline) [1, 2]. Using H₂-powered vehicles could help to meet the 2050 decarbonization target (i.e., zero emissions) [3, 4] set by the European Union [5]. This could be accomplished when H₂ is produced using excess renewable energy sources, and it is easily accessible via a global network of Hydrogen Refuelling Stations (HRSs). HRSs are regarded as one of the most important infrastructures for enabling H₂-fueled vehicles (also referred to as fuel-cell electric vehicles) for sustainable transportation [6, 7]. To utilize H₂ in onboard vehicle tanks, it is compressed up to Normal Working Pressures (NWP) of 70 MPa for Light-Duty Vehicles (LDVs) (i.e., cars) and 35 MPa for Heavy-Duty Vehicles (HDVs) (i.e., trains, aeroplanes, buses, and trucks) permitting a driving range similar to gasoline-powered vehicles [8]. However, compression work during refuelling causes gas within the tank to warm. The onboard vehicle tanks are designed to operate within the gas temperature range of between -40°C and 85°C [9], with the highest filling pressure of 1.25 × NWP i.e. 87.5 MPa (for LDVs) and State of Charge (SOC) of 100% [8, 10]. Beyond these mentioned temperature limits may lead to onboard tank degradation over time and sudden failure of the tank (i.e., H₂ leak or tank rupture) [8, 11]. To prevent vehicle tank overheating, the gas temperature is kept below the 85°C limit

by precooling H₂ to around -40°C using a heat exchanger in the fueling line [12]. To ensure safe refuelling for onboard H₂ cylinders, the Society of Automotive Engineers (SAE) developed the refuelling protocol SAE J2601 [9, 10], which mandates that after filling completion, H₂ cylinders must meet these criteria: temperature below 85°C, maximum pressure permitted 1.25 times the NWP (i.e., 87.5 MPa), and SOC between 90-100% for non-communication fillings. The vehicle tank filling level is determined by the SOC, which represents the ratio of H₂ density within the tank at the end of the refuelling process to its density at 15°C and 70 MPa NWP [9, 10]. One significant barrier preventing H₂ vehicles from being widely adopted is the H₂ storage system. Compressed H₂ storage is currently the most commonly used solution by vehicle manufacturers, utilizing type III and type IV H₂ storage tanks [13]. The type IV tank in particular is an attractive option because of its durability, lightweight design and high volumetric density [14].

Fast filling of onboard H₂ cylinders is essential to achieve the same refuelling time as existing ones. However, rapid filling of the vehicle's H₂ tank can lead to a substantial increase in the temperature inside the tank, posing a significant safety concern. To address this issue, numerous numerical and experimental studies have been conducted to investigate the refuelling process of onboard H₂ tanks in vehicles [15, 16]. Most of the authors such as Galassi et al. [17], Melideo et al. [18], de Miguel et al. [19], and Li et al. [20], developed 2D/3D CFD simulation models to study the impact of various

refuelling parameters on onboard vehicle tanks temperature distribution.

Simulating the entire refilling process or carrying out in-depth parameter studies using 3D CFD simulations is not feasible due to the high computational expenses. Consequently, more straightforward simulation models (0D1D) are needed. The numerical simulation-based H₂ refuelling process models have been widely studied in the published literature [8, 21]. Rothuizen et al. [22], and Schäfer and Klein [23] conducted simulations to optimize HRSs and refuelling processes. The fueling of H₂ from the breakaway to the onboard vehicle storage is performed by Kuroki et al. [24]. A key area of interest for H₂ safety is the investigation of temperature rise during the refuelling process [25]. In this study, a simulation model of HRS for filling a 4 kg-700 bar light-duty H₂ passenger vehicle tank was developed to understand the effect of different refuelling parameters such as H₂ supply or inlet gas temperature and Average Pressure Ramp Rate (APRR), on final vehicle tank temperature and SOC at the end of refuelling process.

2. MODEL DESCRIPTION AND GOVERNING EQUATIONS

Figure 1 presents the schematic representation of the light-duty H₂ vehicle filling process from the refuelling station main storage tank to the onboard H₂ vehicle tank. To simulate the filling process of the vehicle tank, a numerical model has been developed which comprises of following components: one high-pressure main storage tank having 300 liter storage capacity to store H₂ at 900 bar, pipes to connect components, a pressure control valve to reduce the pressure to target pressure, heat exchanger to precool the H₂ temperature to -40°C required temperature for T40 and H70 filling stations [26], breakaway, hose, valves and H₂ IV vehicle tank to store approximately 4 kg of H₂ at 700 bar. The geometric specification and thermal properties for components (breakaway, nozzle, hose) are taken from Kuroki et al. [27], and detailed in Table 1. The pipe size was selected similarly for all the pipes used to connect the components. The brief characteristics of these piping sections are obtained from Kuroki et al. [27], and presented in Table 1.

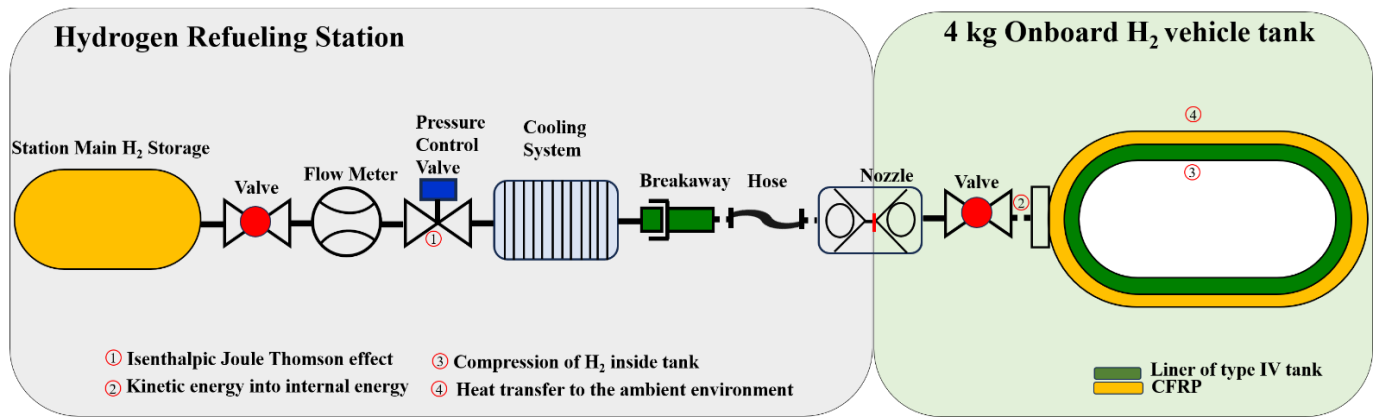


Figure 1. Schematic representation of the model

Table 1. Specifications of components

Component	ID (m)	OD (m)	L (m)	ρ (kg/m ³)	Specific Heat (J/(kg K))	Thermal Conductivity (W/(m K))	Convective Heat Transfer Coefficient (W/(m ² K))
Breakaway	0.00516	0.0383	0.56	7900	659	5	10
Hose	0.00516	0.012	3.5	3694	558	1.5	10
Nozzle	0.00516	0.0388	0.36	7900	659	5	10
Piping Sections							
Pipe (9/16")	0.0079248	0.0142875	3	8000	500	16.3	10

2.1 Governing equations: Onboard vehicle tank

In this work, a pseudo-0D1D modelling approach is employed. The model solves mass and energy balance equations for the entire fueling process and calculates changes in H₂ pressure, temperature, and mass flow rate. It assumes the tank volume remains constant as pressure increases, using preset thermo-mechanical properties. The governing equations for the mass and energy balances are shown as [22, 27]:

$$\frac{d}{dt}[m] = \dot{m}_{in} \quad (1)$$

$$\frac{d}{dt}[mu] = \dot{m}_{in}h_{in} + A_{wall}\alpha_{in}(T_{wall}|_{x=0} - T) \quad (2)$$

where, m represents the H₂ mass in the control volume, meanwhile the u , \dot{m}_{in} , h_{in} , A_{wall} , α_{in} represents the specific internal energy, incoming mass flow rate of the H₂ gas, specific enthalpy at the vehicle tank inlet, tank inner surface area, and tank inner surface heat transfer coefficient respectively. T represents the average H₂ temperature in the onboard tank, $T_{wall}|_{x=0}$ is the inner surface temperature of the tank wall, and t is the time. This model assumes a simplified lumped state inside the tank, treating the temperature and pressure of H₂ as mean values. Heat conduction through the onboard vehicle tank wall is assumed to be one-dimensional, considering a flat plate despite the cylindrical tank shape. This assumption is valid due to the tank's large curvature radius compared to the wall thickness. The model applies an unsteady heat conduction governing equation and boundary conditions to determine the temperature distribution in the tank wall.

$$\frac{\partial T_{wall}}{\partial t} = a_{wall} \frac{\partial^2 T_{wall}}{\partial x^2} \quad (3)$$

$$-\lambda_{wall} \frac{\partial T_{wall}}{\partial x} \Big|_{x=0} = \alpha_{in}(T - T_{wall} \Big|_{x=0}) \quad (4)$$

$$-\lambda_{wall} \frac{\partial T_{wall}}{\partial x} \Big|_{x=l} = \alpha_{out}(T_{wall} \Big|_{x=l} - T_{amb}) \quad (5)$$

where, a_{wall} represents the thermal diffusivity, $x=0$ is the inner wall surface and $x=l$ represents tank wall total thickness, λ_{wall} is the thermal conductivity of the vehicle tank wall, α_{out} represents the outer surface heat transfer coefficient, and T_{amb} is the ambient temperature. The value of α_{out} was set to $8.0W/(K \cdot m^2)$. The value of α_{in} was derived by employing the following correlation equations of Nusselt number [27]:

$$Nu = (Nu_{forced}^4 + Nu_{free}^4)^{0.25} \quad (6)$$

$$Nu_{forced} = 0.17Re^{0.67} \quad (7)$$

$$Nu_{free} = 0.104Ra^{0.352} \quad (8)$$

where, Nu_{forced} and Nu_{free} denote the forced convection and free convection Nusselt number, Re represents the Reynolds number at the onboard storage tank inlet, and Ra depicts the Rayleigh number inside the onboard vehicle tank. After calculating the Nu the α_{in} is calculated by employing the following relationship:

$$Nu = \frac{\alpha_{in}d}{\lambda} \quad (9)$$

where, d and λ represent the internal diameter and H_2 gas thermal conductivity.

2.2 Governing equations: Piping sections, breakaway, hose, and nozzle

The governing equations for the mass and energy balances are shown as follows:

$$\frac{d}{dt}[m] = \dot{m}_{in} - \dot{m}_{out} \quad (10)$$

$$\frac{d}{dt}[mu] = \dot{m}_{in}h_{in} - \dot{m}_{out}h_{out} + q_{in}A_{wall} \quad (11)$$

where, q_{in} denote the the heat flux that is transmitted from the HRS main component's wall to H_2 . To calculate the value of the q_{in} the following unsteady governing heat equation is solved.

$$\frac{\partial T_{wall}}{\partial t} = a_{wall} \left(\frac{\partial^2 T_{wall}}{\partial r^2} + \frac{1}{r} \frac{\partial T_{wall}}{\partial r} \right) \quad (12)$$

$$q_{in} = -\lambda_{wall} \frac{\partial T_{wall}}{\partial x} \Big|_{r=r_{in}} = \alpha_{in}(T - T_{wall} \Big|_{r=r_{in}}) \quad (13)$$

$$q_{out} = \alpha_{out}(T_{wall} \Big|_{r=r_{out}} - T_{amb}) \quad (14)$$

where, r denotes the position or location in the radial direction at which r_{in} and r_{out} are inner and outer surfaces. For the outer surface, the value of the heat transfer coefficient was

selected as $8.0W/(K \cdot m^2)$, and the value of the inner surface heat transfer coefficient is obtained by employing the Nusselt number equation.

$$Nu_{free} = 0.022Re^{0.8}Pr^{0.5} \quad (15)$$

2.3 Governing equations: Valves and mass flow rate

Volumetric flow rate (m^3/h) calculation: calculates the volumetric flow rate based on the differential pressure at the inlet and outlet of the valve ($P_{upstream}$ or P_i and $P_{downstream}$ or P_{i+1}), the temperature at the inlet of the valve $T_{upstream}$, and specific gravity to air G_i . If $P_{upstream} \geq 0.5 * P_{downstream}$ (non-choked flow) [24, 27]:

$$\dot{V} = 2940Cv \sqrt{\frac{(P_i - P_{i+1})(P_i + P_{i+1})}{P_i G_i T_i}} \quad (16)$$

If $P_{upstream} < 0.5 * P_{downstream}$ (choked flow):

$$\dot{V} = 2538Cv \frac{P_i}{\sqrt{G_i T_i}} \quad (17)$$

Conversion to mass flow rate (kg/s): Converts the volumetric flow rate (m^3/h) to the mass flow rate (kg/s) using density at 0.1MPa and 15.6°C and a coefficient β , developed to handle the unsteady flow during the fueling process:

$$\dot{m} = \frac{\beta \rho \dot{V}}{3600} \quad (18)$$

where, ρ is H_2 density at 0.1MPa and 15.6°C and the correction coefficient β is shown in Eq. (18) as a function of H_2 gas density on the upstream side and the volumetric flow rate:

$$\beta = 7.0 \times 10^{-3} \dot{V} + (0.04 \rho_i)^{1.75} \quad (19)$$

The H_2 filling process manages irregular flows where the mass flow rate fluctuates or varies within an estimated range of 0.0 to 60.0g/s.

3. MODEL ASSUMPTIONS

The following assumptions have been used to develop the refuelling model of an HRS for fast filling of light-duty passenger vehicles of 4 kg tank capacity for NWP of 70MPa. The H_2 gas in the station's main storage tank and onboard vehicle tank are considered to be uniformly mixed. The thermodynamic state of H_2 gas in each piping section is assumed to be identical and heat conduction through the walls of the pipe is neglected. Before filing the vehicle tank, the initial temperature of all components is considered to be at ambient temperature [27]. Simulating a complete refuelling station process is challenging and it requires an understanding of both the H_2 thermodynamic properties and the component's material properties across the temperature and pressure range of fueling. The work of Sakoda et al. [28] provides a general summary of the available Equation of States (EOSs) for H_2 . In this present work, after setting the component's initial temperature and pressure the viral EOS by Sakoda et al. [29], for high-pressure H_2 is used to compute specific internal energy, density and enthalpy for each component [27].

4. MODEL VALIDATION

The H₂ fueling thermodynamic model was validated using the experimental and simulation data reported by Kuroki et al. [27]. The specifications of HRS components such as storage tanks, pipes, valves, cooling systems, nozzle, breakaway and hose are obtained from the same work [27]. The model validation only considers the onboard vehicle tank main fuelling event, excluding initial tank pulses and leak checks. Simulation results of the model are compared with the data presented in Ref. [27]. to examine the correctness of the model.

Table 2. Specifications and thermal properties of 4 kg type sIV tank

Parameter	Value	Unit
Initial vehicle tank temperature	20	°C
Initial vehicle tank pressure	5	MPa
Inside surface area	1.1	m ²
Internal volume	99	liters
Tank length	0.855	m
Internal diameter	0.42	m
Liner thickness	0.005	m
Liner density	945	kg/m ³
Liner thermal conductivity	0.5	W/m K
Liner specific heat	2100	J/kg K
Composite thickness	0.0316	m
Composite density	1494	kg/m ³
Composite thermal conductivity	0.5	W/m K
Composite specific heat	1120	J/kg K
Outer surface convective heat transfer coefficient	8	W/m ² K

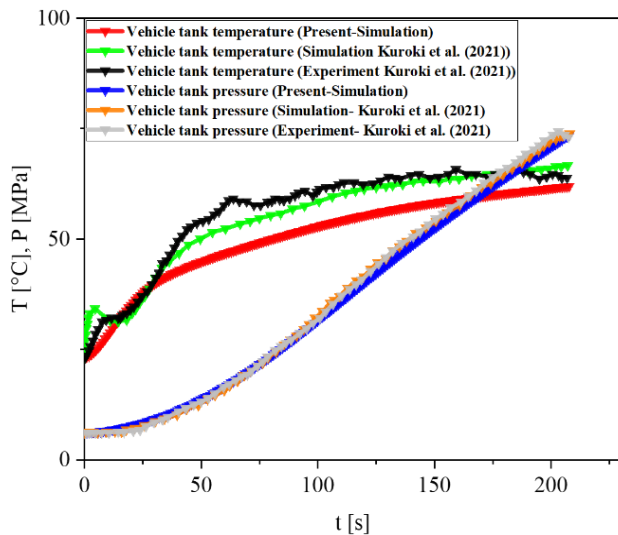


Figure 2. Comparison between experimental and present simulated results of onboard vehicle tank pressure and temperature [27]

5. RESULTS AND DISCUSSION

The refuelling simulation was carried out by considering initial and simulation boundary conditions which are given as; simulation termination condition was selected at 74.5MPa and a constant Average Pressure Ramp Rate (APRR) of 21.8MPa was set to satisfy the 3 minutes refuelling from the lowest initial vehicle tank pressure (5MPa) to maximum allowable onboard tank pressure of 87.5MPa for light-duty passenger vehicles. The ambient temperature of all the components such as the main storage tank, PCV, heat exchanger, piping sections

Simulation boundary conditions for the model are set based on the SAE J2601 [26] standard data provided for non-communication filling. The simulation is conducted using a 99-liter vehicle tank with a NWP 70 MPa. Table 2 shows the thermal properties and specifications of the onboard vehicle tank which are obtained from SAE J2601 protocol data [26]. As shown in Figure 2, the vehicle tank pressure and temperature profiles from the developed model are in good agreement with experimental data conducted by Kuroki et al. [27].

and all the valves employed in the fueling line is considered as 20°C and the initial vehicle tank temperature is also set as 20°C. The incoming gas temperature at the heat exchanger outlet was chosen as -40°C, as suggested by the SAE J2601 refuelling standard [26] for non-communication fillings.

5.1 Effects of H₂ supply temperature on fueling performance and SOC

Figure 3(a), shows the effect of different H₂ supply temperatures (inlet gas temperature) on the vehicle tank temperature and SOC. Precooling H₂ gas up to -40°C before fueling it into a vehicle tank is an effective way to meet the safety requirement set by the SAE J2601 standard [26]. As shown in Figure 3(a), the maximum temperature of the vehicle cylinder reaches 113.8°C for an inlet gas temperature of 20°C and it decreases to 68.9°C when H₂ is precooled to the temperature of -40°C. Furthermore, a higher inlet gas temperature also reduces the gas density inside the cylinder, resulting in a reduction of the final mass delivery. Generally, the total quantity of H₂ stored in the vehicle cylinder is measured using the so-called State of Charge (SOC). SOC is the ratio of H₂ density after refuelling to a reference density at 15°C and NWP 70MPa for type IV tanks. The SOC can be calculated by given Eq. (20) [30].

$$SOC = \frac{\rho_{H_2} (T_{final}, P_{final})}{\rho_{H_2} (15^\circ C, 70MPa)} \quad (20)$$

According to the study conducted by Schneider et al. [30], the SAE J2601 minimum allowed SOC value for an HRS, without communication filling between the tank and dispenser, is 90%. Figure 3(b) demonstrates how incoming gas temperature affects the vehicle tank's ultimate SOC. The higher the temperature of the H₂ gas, the lower the gas density

at the end of the refuelling procedure. The SOC decreases as the final gas temperature increases. Figure 3(b) shows that SOC reaches a remarkable peak of 92.2% at -40°C for precooled H_2 gas, but decreases to 84.6% at 20°C .

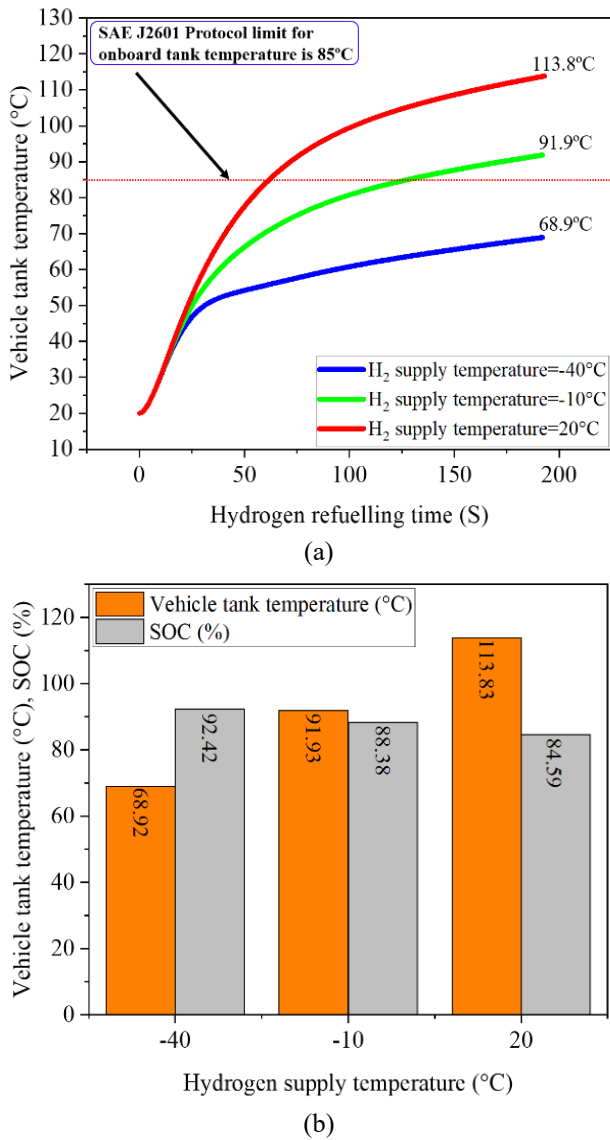


Figure 3. Effect of H_2 supply temperature on (a) vehicle tank temperature (b) SOC

5.2 Effects of APRR on fueling performance and SOC

Simulations were performed to examine the effect of APRRs of 5MPa/min, 21.8MPa/min (base case), and 50MPa/min on vehicle fueling performance and the final SOC of the tank. As shown in Figure 4(a), the vehicle tank temperature increases from 61.19°C to 74.26°C as the APRR increases from 5MPa/min to 50MPa min. Higher APRR, as predicted, raises the average refuelling mass flow rate and it shortens the time required to reach maximum SOC at the end of the onboard tank fill. Increasing mass flow rate leads to an increase in energy flow rate in the H_2 vehicle cylinder, in the form of specific gas kinetic energy and enthalpy. As a result of the higher energy rate, the tank temperature rises more quickly. Filling an onboard vehicle tank with an increased fueling rate by enhanced APRR leads to higher-end fill temperature due to the tank wall's higher thermal resistance and slow heat dissipation rate to the environment. Figure 4(b)

depicts the vehicle tank final SOC at various APRRs. It can be seen from Figure 4(b), that SOC reaches a maximum of 94.19% at APRR 5MPa/min and it reduces to 91.12% for the higher APRRs. Lower APRR is preferable, since it requires less cooling capacity, allowing for maximum SOC even when employing higher precooling temperatures. Longer fuelling times, however, are caused by reduced APRR, which could have an impact on consumer satisfaction because lower APRR increases the total time to fill the vehicle tank. For instance, Figure 4(b) demonstrates that 94.2% SOC may be achieved at 5.0MPa/min APRR, However, the fill time would be slightly more over 13 minutes for a 4 kg filling tank.

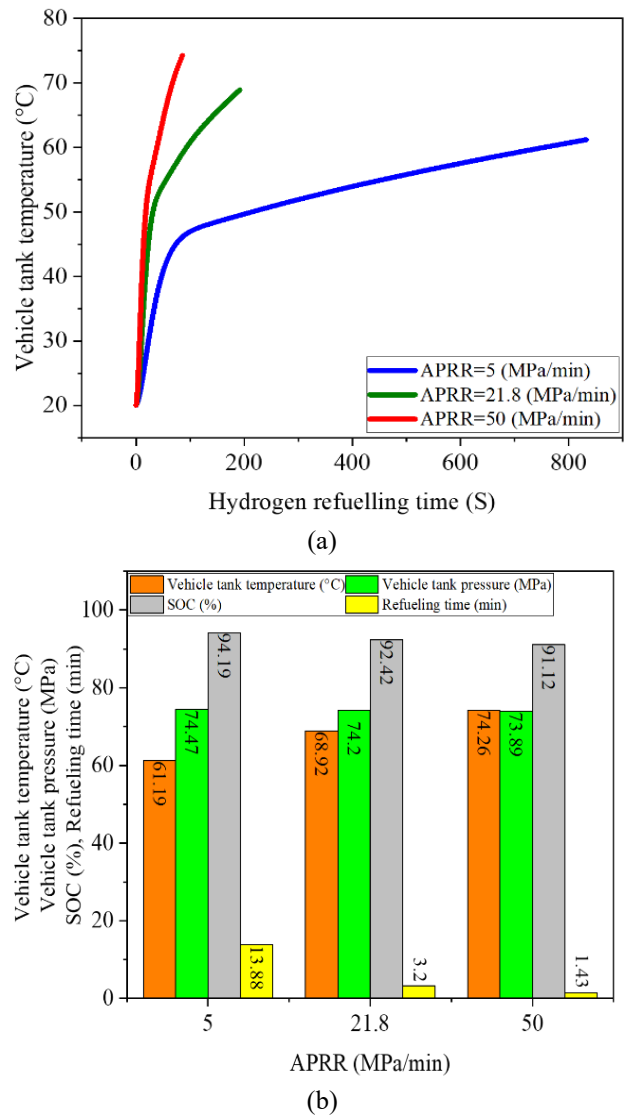


Figure 4. Effect of APRR on (a) vehicle tank temperature (b) SOC

6. CONCLUSIONS

In this study, a numerical simulation model was developed to examine the refuelling process and evaluate the final state of charge for light-duty vehicles equipped with a 4 kg gas capacity tank. The model takes into consideration filling an NWP 700MPa type IV tank at 20°C ambient temperature and initial pressure of 5MPa. Through simulations, the impact of different refuelling parameters on the state of charge (SOC) of the vehicle's tank and the effectiveness of refuelling has been

examined. These parameters include the temperature of the incoming gas and the APRR. The purpose of the simulations is to determine how these refuelling parameters affect the refuelling process's efficiency and ultimate SOC. The findings revealed that the inlet gas temperature has a remarkable effect on the final vehicle tank temperature and SOC. The simulation results indicate that raising the inlet gas temperature from -40°C to 20°C leads to a substantial increase in the final vehicle tank temperature from 68.9°C to 113.8°C. Additionally, the SOC of the tank decreases by 9.3% from 92.4% to 84.6% as a result of this temperature increase.

REFERENCES

- [1] Battaglia, V., Vanoli, L. (2024). Power-to-X strategies for smart energy regions: A vision for green hydrogen valleys. *Energy Efficiency*, 17(3): 14. <https://doi.org/10.1007/s12053-024-10194-0>
- [2] Nocera, S., Cavallaro, F. (2016). The competitiveness of alternative transport fuels for CO₂ emissions. *Transport Policy*, 50: 1-14. <https://doi.org/10.1016/j.tranpol.2016.05.013>
- [3] Di Fraia, S., Di Meglio, A., Massarotti, N., Vanoli, L., Bentivoglio, R., Volpecina, V. (2024). Energy recovery and waste valorization in a frozen food processing facility: A case study from Lazio, Italy. *Energy Efficiency*, 17(3): 13. <https://doi.org/10.1007/s12053-024-10193-1>
- [4] Battaglia, V., De Luca, G., Fabozzi, S., Lund, H., Vanoli, L. (2022). Integrated energy planning to meet 2050 European targets: A Southern Italian region case study. *Energy Strategy Reviews*, 41: 100844. <https://doi.org/10.1016/j.esr.2022.100844>
- [5] Perissi, I., Jones, A. (2022). Investigating European union decarbonization strategies: Evaluating the pathway to carbon neutrality by 2050. *Sustainability*, 14(8): 4728. <https://doi.org/10.3390/su14084728>
- [6] Mahmood, M.A., Chaudhary, T.N., Farooq, M., Habib, M.S., Maka, A.O., Usman, M., Sultan, M., Lam, S.S., Chen, B. (2023). Sensitivity analysis of performance and thermal impacts of a single hydrogen fueled solid oxide fuel cell to optimize the operational and design parameters. *Sustainable Energy Technologies and Assessments*, 57: 103241. <https://doi.org/10.1016/j.seta.2023.103241>
- [7] Chaudhary, T.N., Akbar, A., Usman, M., Mahmood, M.A., Maka, A.O., Chen, B. (2023). Parametric sensitivity analysis to investigate the effects of operating and design parameters on single direct methane steam reforming solid oxide fuel cell performance and thermal impacts generation. *Energy Conversion and Management*, X, 18: 100374. <https://doi.org/10.1016/j.ecmx.2023.100374>
- [8] Molkov, V., Ebne-Abbasi, H., Makarov, D. (2023). CFD model of refuelling through the entire HRS equipment: The start-up phase simulations. *Hydrogen*, 4(3): 585-598. <https://doi.org/10.3390/hydrogen4030038>
- [9] SAE International Technical Standard. Fueling Protocols for Light Duty Gaseous Hydrogen Surface Vehicles, SAE Standard J2601_201612, 2010. https://doi.org/10.4271/J2601_201612
- [10] SAE International Technical Standard. Fueling Protocols for Light Duty Gaseous Hydrogen Surface Vehicles, SAE Standard J2601_202005, 2010. https://doi.org/10.4271/J2601_202005
- [11] Bagarello, S., Campagna, D., Benedetti, I. (2024). A survey on hydrogen tanks for sustainable aviation. *Green Energy and Intelligent Transportation*, 100224. <https://doi.org/10.1016/j.geits.2024.100224>
- [12] Nanmaran, R., Mageswari, M., Srimathi, S., Raja, G.G., Al Obaid, S., Alharbi, S.A., Elumalai, P., Thanigaivel, S. (2024). Mathematical modelling of hydrogen transportation from reservoir tank to hydrogen fuel cell electric vehicle (FCEV) tank. *Fuel*, 361: 130725. <https://doi.org/10.1016/j.fuel.2023.130725>
- [13] Gómez, J.A., Santos, D.M. (2023). The status of on-board hydrogen storage in fuel cell electric vehicles. *Designs*, 7(4): 97. <https://doi.org/10.3390/designs7040097>
- [14] Rivard, E., Trudeau, M., Zaghbi, K. (2019). Hydrogen storage for mobility: A review. *Materials*, 12(12): 1973. <https://doi.org/10.3390/ma12121973>
- [15] Zhao, B., Wei, H., Peng, X., Feng, J., Jia, X. (2022). Experimental and numerical research on temperature evolution during the fast-filling process of a type III hydrogen tank. *Energies*, 15(10): 3811. <https://doi.org/10.3390/en15103811>
- [16] Park, B.H., Lee, D.H. (2022). Flow analysis and development of a model to simulate transient temperature of hydrogen from pre-cooler to on-board storage tank during hydrogen refueling. *Korean Journal of Chemical Engineering*, 39(4): 902-912. <https://doi.org/10.1007/s11814-022-1085-4>
- [17] Galassi, M.C., Baraldi, D., Iborra, B.A., Moretto, P. (2012). CFD analysis of fast filling scenarios for 70MPa hydrogen type IV tanks. *International Journal of Hydrogen Energy*, 37(8): 6886-6892. <https://doi.org/10.1016/j.ijhydene.2012.01.041>
- [18] Melideo, D., Baraldi, D., Acosta-Iborra, B., Cebolla, R.O., Moretto, P. (2017). CFD simulations of filling and emptying of hydrogen tanks. *International Journal of Hydrogen Energy*, 42(11): 7304-7313. <https://doi.org/10.1016/j.ijhydene.2016.05.262>
- [19] de Miguel, N., Acosta, B., Baraldi, D., Melideo, R., Cebolla, R.O., Moretto, P. (2016). The role of initial tank temperature on refuelling of on-board hydrogen tanks. *International Journal of Hydrogen Energy*, 41(20): 8606-8615. <https://doi.org/10.1016/j.ijhydene.2016.03.158>
- [20] Li, J., Wang, T., Yang, Q., Song, P., Su, H. (2023). Towards fast and safe hydrogen filling for the fuel vehicle: A variable mass flow filling strategy based on a real-time thermodynamic model. *International Journal of Hydrogen Energy*, 48(53): 20406-20418. <http://doi.org/10.1016/j.ijhydene.2023.03.001>
- [21] Zhao, Y., Liu, G., Liu, Y., Zheng, J., Chen, Y., Zhao, L., Guo, J., He, Y. (2012). Numerical study on fast filling of 70 MPa type III cylinder for hydrogen vehicle. *International Journal of Hydrogen Energy*, 37(22): 17517-17522. <https://doi.org/10.1016/j.ijhydene.2012.03.046>
- [22] Rothuizen, E., Elmegaard, B., Rokni, M. (2020). Dynamic simulation of the effect of vehicle-side pressure loss of hydrogen fueling process. *International Journal of Hydrogen Energy*, 45(15): 9025-9038. <https://doi.org/10.1016/j.ijhydene.2020.01.071>
- [23] Schäfer, S., Klein, H. (2019). Thermodynamical analysis of a hydrogen fueling station via dynamic simulation.

- International Journal of Hydrogen Energy, 44(33): 18240-18254.
<https://doi.org/10.1016/j.ijhydene.2019.04.144>
- [24] Kuroki, T., Sakoda, N., Shinzato, K., Monde, M., Takata, Y. (2018). Dynamic simulation for optimal hydrogen refueling method to Fuel Cell Vehicle tanks. International Journal of Hydrogen Energy, 43(11): 5714-5721. <https://doi.org/10.1016/j.ijhydene.2018.01.111>
- [25] Monde, M., Kosaka, M. (2013). Understanding of thermal characteristics of fueling hydrogen high pressure tanks and governing parameters. SAE International Journal of Alternative Powertrains, 2(1): 61-67. <https://doi.org/10.4271/2013-01-0474>
- [26] SAE International Technical Standard. Fueling Protocols for Light Duty Gaseous Hydrogen Surface Vehicles, SAE Standard J2601_202005, 2016. https://doi.org/10.4271/J2601_202005
- [27] Kuroki, T., Nagasawa, K., Peters, M., Leighton, D., Kurtz, J., Sakoda, N., Monde, M., Takata, Y. (2021). Thermodynamic modeling of hydrogen fueling process from high-pressure storage tank to vehicle tank. International Journal of Hydrogen Energy, 46(42): 22004-22017. <https://doi.org/10.1016/j.ijhydene.2021.04.037>
- [28] Sakoda, N., Shindo, K., Shinzato, K., Kohno, M., Takata, Y., Fujii, M. (2010). Review of the thermodynamic properties of hydrogen based on existing equations of state. International Journal of Thermophysics, 31: 276-296. <https://doi.org/10.1007/s10765-009-0699-7>
- [29] Sakoda, N., Shindo, K., Motomura, K., Shinzato, K., Kohno, M., Takata, Y., Fujii, M. (2012). Burnett PVT measurements of hydrogen and the development of a virial equation of state at pressures up to 100MPa. International Journal of Thermophysics, 33: 381-395. <https://doi.org/10.1007/s10765-012-1168-2>
- [30] Schneider, J., Meadows, G., Mathison, S.R., Veenstra, M.J., Shim, J., Immel, R., Wistoft-Ibsen, M., Quong, S., Greisel, M., McGuire, T., Potzel, P. (2014). Validation and sensitivity studies for SAE J2601, the light duty vehicle hydrogen fueling standard. SAE International Journal of Alternative Powertrains, 3(2): 257-309. <https://doi.org/10.4271/2014-01-1990>